

## Diffusion of organic anions in clay-rich mediaeffect of porosity exclusion on retardation

R.H. Dagnelie, S. Rasamimanana, V. Blin, J. Radwan, E. Thory, J-C. Robinet, G. Lefevre

► **To cite this version:**

R.H. Dagnelie, S. Rasamimanana, V. Blin, J. Radwan, E. Thory, et al.. Diffusion of organic anions in clay-rich mediaeffect of porosity exclusion on retardation. Chemosphere, Elsevier, 2018, 10.1016/j.chemosphere.2018.09.064 . cea-02339780

**HAL Id: cea-02339780**

**<https://hal-cea.archives-ouvertes.fr/cea-02339780>**

Submitted on 5 Nov 2019

**HAL** is a multi-disciplinary open access archive for the deposit and dissemination of scientific research documents, whether they are published or not. The documents may come from teaching and research institutions in France or abroad, or from public or private research centers.

L'archive ouverte pluridisciplinaire **HAL**, est destinée au dépôt et à la diffusion de documents scientifiques de niveau recherche, publiés ou non, émanant des établissements d'enseignement et de recherche français ou étrangers, des laboratoires publics ou privés.

1 Diffusion of organic anions in clay-rich media:  
2 effect of porosity exclusion on retardation  
3

4 R.V.H. Dagnelie<sup>(a,\*)</sup>, S. Rasamimanana<sup>(a)</sup>, V. Blin<sup>(a)</sup>, J. Radwan<sup>(a)</sup>,  
5 E. Thory<sup>(a)</sup>, J.-C. Robinet<sup>(b)</sup>, G. Lefèvre<sup>(c)</sup>  
6

7 <sup>(a)</sup>DEN-Service d'Etude du Comportement des Radionucléides (SECR),  
8 CEA, Université Paris-Saclay, F-91191 Gif-sur-Yvette, France

9 <sup>(b)</sup> Andra, R&D Division, parc de la Croix Blanche, 92298, Châtenay-Malabry, France

10 <sup>(c)</sup>PSL Research University, Chimie ParisTech-CNRS, Institut de Recherche de Chimie Paris,  
11 11 rue Pierre et Marie Curie, F-75005 Paris, France  
12  
13  
14  
15  
16  
17  
18

19 \* Corresponding author: R.V.H. Dagnelie, [romain.dagnelie@cea.fr](mailto:romain.dagnelie@cea.fr), Tel: +33 (0)1 69 08 50 41

### Highlights

- 1 Retarded diffusion of organic anions was studied in Callovo-Oxfordian claystone
- 2 Charge and or steric effects lead to strongly reduced apparent porosity for carboxylic acids
- 3 This exclusion lowers simultaneously porosity, effective diffusion and retardation
- 4 A correction factor is proposed with a retardation collapse below a threshold:  $\varepsilon_a/\varepsilon < b$
- 5 A methodology is proposed to evaluate retardation of organic anions in claystones

## 20 **Abstract**

21           The adsorption of solutes in porous rocks and soils is known to induce retardation  
22 during transport. We studied the case of diffusion of organic anions in a clay rich media, for  
23 which a discrepancy was previously observed between adsorption measured by batch and  
24 diffusion experiments. Organic anions display an affinity with clay and oxides surfaces  
25 leading to adsorption. However, they are subject to a partial exclusion from porosity ( $\epsilon_a < \epsilon$ ),  
26 because of steric and charge effects. We evaluated the possible correlation between the  
27 decrease of accessible porosity and a decrease of diffusive retardation. An empirical  
28 correction factor was proposed to explain the difference between maximum and apparent  
29 adsorption, respectively measured by batch and diffusion experiments. This correction was  
30 evaluated for Callovo-Oxfordian clay rock and used to interpret 15 diffusion experiments. A  
31 reasonable agreement was observed between adsorption isotherms from batch and corrected  
32 values from diffusion experiments. A low diffusivity of organic species in Callovo-Oxfordian  
33 was confirmed, with  $D_e$  values ranging between 0.5 and  $7 \cdot 10^{-12} \text{ m}^2 \text{ s}^{-1}$ , indicating anion  
34 exclusion. Still a significant retardation was observed for species such as oxalate, citrate or  $\alpha$ -  
35 isosaccharinate. This retardation factor decreases with accessible porosity, with a threshold  
36 value observed when  $\epsilon_a/\epsilon < 0.65$ . This feature has strong implications for estimation of  
37 migration parameters of solutes in the environment. The proposed methodology would be  
38 suitable for other media with charged surfaces such as cementitious materials or oxisoils.

## 39 **1. Introduction**

40           Organic molecules are widely studied in environmental sciences such as pedology,  
41 geology or marine chemistry. Among them, organic pollutants such as anthropogenic organic  
42 matter (AOM) can be potentially released from hazardous waste and migrate through  
43 geological rock formation or soils (Duarte et al., 2018). AOM refers to a wide range of  
44 compounds, including polar and apolar molecules, ionic and neutral molecules. The ionic  
45 polar molecules are highly soluble in water and more mobile in soils and rocks (Schaffer and  
46 Licha, 2015). The neutral (poly)aromatic compounds are less soluble, often absorbed by soil  
47 organic matter (Borisover and Graber, 1997), but also more resistant against (bio)degradation  
48 (Ren et al., 2018). For all these compounds, sorption processes slow down their migration in  
49 environmental conditions (Curtis et al., 1986; Weber et al., 1991). Consequently,  
50 understanding retardation phenomena of soluble organic matter is crucial for bioavailability of  
51 solutes, remediation of soils, extraction of ore, or hazardous waste management. Several  
52 scientific communities have investigated such issues for specific media (soils, sand,  
53 sedimentary rocks, cement based materials...) or site specific conditions (acidic, neutral or  
54 alkaline, oxidant or reducing media...). For example, the migration of organic ligands was  
55 largely investigated in many oxide-rich soils and model materials (Liu et al., 2014). In this  
56 field, a good agreement is usually observed between adsorption measured by batch  
57 experiments, results from flow-through methods and field observations (Liu et al., 2013;  
58 Banzhaf and Hebig, 2016). Such approach requires determining and studying the relevant  
59 factors controlling site-specific transport, for example adsorption-dissociation processes  
60 (Zachara et al., 1995; Szecsody et al., 1998), slow kinetics-driven transport (Brusseau, 1991),  
61 colloidal effects (Roy and Dzombak, 1998), etc. Similar issue was recently raised for  
62 diffusion of organic anions in clay-rich rocks (Durce et al., 2014; Dagnelie et al., 2014).

63 In the past decade, a tremendous effort was made to study solutes migration  
64 phenomena in geological media in the context of deep underground radioactive wastes  
65 repository (Altman et al., 2012; Tournassat et al., 2015). Sedimentary clay rich rocks, such as  
66 the Callovo-Oxfordian mudstone (France), Boom clays (Belgium), Opalinus clays  
67 (Switzerland) were intensively studied in this context (Delage et al., 2010). They are  
68 characterized by low hydraulic conductivities and diffusion coefficients due to their narrow  
69 pore network and by high retention properties of cations due their affinity with the  
70 constituting clay minerals. In such rocks, the migration of cations is mainly driven by their  
71 adsorption on clay minerals (Melkior et al., 2007; Savoye et al., 2012; 2015). On the contrary,  
72 inorganic anions display a poor affinity for clay surfaces and they are repelled from the pore  
73 surface leading to the well-established “anion exclusion” phenomena (Bazer-Bachi et al.,  
74 2007; Descostes et al., 2008; Frasca et al., 2012; Montavon et al., 2014). The behaviour of  
75 small organic anions was found to be intermediate between those of cations and inorganic  
76 anions (Dagnelie et al., 2014). Small carboxylates are affected by “anion exclusion” as  
77 inorganic anions and displays retention properties as inorganic cations (Descostes et al.,  
78 2017). These compounds are studied for various safety assessments, including metal and  
79 radionuclides transport (Nowack et al., 1997; Read et al., 1998; Hummel, 2008; Charlet et al.,  
80 2017). Rasamimanana et al. (2017a) recently quantified and summarized the adsorption of  
81 various carboxylic anions (acetate, phthalate, citrate), deduced from batch experiments on  
82 Callovo-Oxfordian mudstone. Solid to liquid distribution coefficient ( $R_d$ ) are ranged from 0.1  
83 to several tens of  $L.kg^{-1}$  demonstrating the significant affinity of the rock for these anions.  
84 Similar trends were recently confirmed by percolation experiments on compacted illite with  
85 hydrophilic hydroxyl-acids (Chen et al., 2018). Yet a key point remains unclear for organic  
86 anions, which is the discrepancy between high  $R_d$  values measured by batch experiments and  
87 low retardation factors measured by migration experiments (Dagnelie et al, 2014). The origin

88 of this discrepancy has to be cleared in order to predict the reactive transport of organics, as  
89 correctly achieved for other solutes.

90 The objective of this work was to evaluate the diffusive behaviour of various organic  
91 anions in a clay-rich sedimentary rock and compare diffusive retardation factors with  
92 adsorption data. This was performed in Callovo-Oxfordian clay rock, for which a clear picture  
93 of anion adsorption was available in the literature. A possible explanation is provided for the  
94 discrepancies previously observed between batch and diffusion experiments.

95

## 96 **2. Material and methods**

### 97 **2.1 Rock samples**

98 Experiments were carried out on samples originated from the Callovo-Oxfordian  
99 sedimentary formation (Meuse/Haute-Marne France). The rock cores, EST40471 and  
100 EST207\_16517 and EST\_16520, were drilled from a borehole in the underground laboratory  
101 at -501 m and -498 m in depth from the surface respectively. The claystone comes from the  
102 clayey unit constituted of clayey unit constituted by 50-55% of clay minerals (illite,  
103 interlayered illite-smectite, kaolinite, chlorite), 18 -20% of tectosilicates (mainly quartz), 22-  
104 35 % of carbonates (mainly calcite) and less than 5 % of accessory minerals (pyrite, iron  
105 oxide...). Organics matter is estimated to < 1% (COT ~ 0.6%) (Gaucher et al., 2004; Lerouge  
106 et al., 2011; Pellenard et al., 2014). The core sample was protected from O<sub>2</sub> after drilling  
107 using container under N<sub>2(g)</sub>. Thanks to a wire saw inside a glovebox, the rock core were sliced  
108 into ~10 mm thick samples and then adjusted to 35 - 40 mm of diameter. The dimension of  
109 the samples is listed in supplementary data (Table S1). The weighting of solid samples led to  
110 an average hydrated density  $\rho_H \sim 2.34 \pm 0.06 \text{ g cm}^{-3}$  leading to a total porosity of 21 %  
111 assuming a grain density,  $\rho_g \sim 2.7 \text{ g cm}^{-3}$  ( $\epsilon \sim [\rho_H - \rho_g] / [1 - \rho_g]$ ).

112

## 113 2.2 Diffusion experiments

114 Two main setups were used in this study and displayed a good repeatability (Table  
115 S1). The static setup includes a PEEK cell, a sample pasted with epoxy resin between two  
116 filterplates in contact with upstream / downstream solutions (see Descostes et al., 2008 for  
117 detailed setup). The dynamic setup includes a stainless steel cell, a sample swelled inside the  
118 cell without filterplates or resin, and in contact with solutions circulating in upstream /  
119 downstream reservoirs (see Savoye et al., 2011 for detailed setup). The list of diffusion  
120 experiments is detailed in Table 1, including each organic tracer monitored. Table 1 mostly  
121 gathers experimental results, including the diffusion data of organic tracers and when  
122 available, the diffusion data of inert tracers (HTO, HDO) used prior to experiments with  
123 organics. Complementary information is available in supplementary data (Table S1): size,  
124 activities, concentration, ionic strength. Experiments n°8 and 10 were performed in presence  
125 of competing solute, respectively  $[\text{Na}_2\text{Phthalate}] = 10^{-1}$  M and  $[\text{NaISA}] = 10^{-2}$  M. The effect  
126 of these competing anions and of ionic strength will also be discussed furtherly.

127

## 128 2.3 Modelling

129 The solid to solution distribution ratio is noted  $R_d$  ( $\text{L.kg}^{-1}$ ). It is defined and modelled by

$$130 R_d = \frac{C_{ads}}{C_e} \quad R_d(C_e) = \frac{K_L \times Q}{(1 + K_L \times C_e)} \quad (1)$$

131 where  $C_{ads}$  ( $\text{mol kg}^{-1}$ ) is the concentration of adsorbed species per mass of adsorbent, and  
132  $C_e$  ( $\text{mol L}^{-1}$ ) the concentration in solution at equilibrium with the solid. The adsorption  
133 isotherms,  $R_d(C_e)$ , displayed a Langmuir-Type shape (Eq. 1) and parameters ( $K_L$ ,  $Q$ ) were  
134 quantified by Rasamimanana et al. (2017). The analysis of the through-diffusion results,  
135 which is based on Fick's second law:

$$136 \frac{\partial C}{\partial t} = \frac{D_e}{\varepsilon_a + \rho_g(1-\varepsilon)R_d^{APP}} \frac{\partial^2 C}{\partial x^2} = \frac{D_e}{\alpha} \frac{\partial^2 C}{\partial x^2} \quad (2)$$



137 with  $C$  representing the tracer concentration ( $\text{mol m}^{-3}$ ),  $t$  the time (s),  $D_e$  the effective  
 138 diffusion coefficient ( $\text{m}^2 \text{s}^{-1}$ ),  $\varepsilon_a$  the diffusion-accessible porosity,  $\rho_g$  the grain density ( $\sim 2.7$   
 139  $\text{kg L}^{-1}$ ),  $R_d^{\text{APP}}$  the apparent adsorption coefficient, and  $\alpha$  the rock capacity factor.  $R = \alpha/\varepsilon_a$  is  
 140 usually called the retardation factor. The initial conditions were  $C(x=0) = C_0$ ,  $C(x \neq 0) = 0$ .  
 141 Fully analytical solutions were performed to fit the results with a constant  $R_d^{\text{APP}}$  value. The  
 142 resolution was performed by numerical resolution in the Laplace space (Crank, 1975;  
 143 Moridis, 1998). The downstream flux of tracer,  $J$  ( $\text{moles m}^{-2} \text{s}^{-1}$ ) was defined by equation (3):  
 144

$$145 \quad J_{down}(t) = \frac{dn_{down}(t)}{S \times dt} = \frac{V_{down}}{S} \lim_{\Delta t \rightarrow 0} \frac{C_{down}(t + \Delta t) - C_{down}(t - \Delta t)}{2 \times \Delta t} \quad (3)$$

146  
 147 where  $dn_{down}$  is the quantity of tracer reaching the downstream compartment in (moles or Bq),  
 148 per unit of time,  $dt$  (s), and sample surface  $S$  ( $\text{m}^2$ ).  $V_{down}$  ( $\text{m}^3$ ) is the downstream volume and  
 149  $\Delta t$  the duration between two successive measurements. In the case of experimental data,  $C_{down}$   
 150 ( $\text{mol L}^{-1}$ ) was corrected from radioactive decay and sampling, and named cumulative  
 151 concentration. All results are discussed on the basis of a normalised flux of tracer:

$$152 \quad \text{NORM} J_{down}(t) = \frac{L}{C_0} J_{down}(t) \quad (4)$$

153 with  $L$  (m) being the sample width and  $C_0$  ( $\text{moles m}^{-3}$ ) the initial concentration of tracer in  
 154 upstream reservoir. By using  $\text{NORM} J_{down}$  ( $\text{m}^2 \text{s}^{-1}$ ), the direct comparison of the different  
 155 experiments was possible, regardless of  $C_0$  or  $L$ . Experiments tend to move towards a  
 156 stationary state where the flux is close to the effective diffusion coefficient  $\text{NORM} J_{DOWN}(t \rightarrow \infty)$   
 157  $\sim D_e$ , as long as upstream and downstream concentrations evolve slowly,  $(C_{up} - C_{down})(t \rightarrow \infty) \sim$   
 158  $C_0$ .

159 The two parameters  $D_e$  and  $\alpha$  were adjusted by least-square fitting of experimental  
 160 normalized downstream flux with a weighting inversely proportional to the experimental

161 precision. The upstream concentration was not used at all for adjustment. This choice was  
162 made because specific effects (perturbation of speciation, non-reversible adsorption, slow  
163 kinetics) might lead to uncomplete mass balance between upstream and downstream  
164 measurements (Roberts et al., 1986). A good agreement between upstream experimental data  
165 and the modelling (adjusted on downstream data) only strengthens the reliability of the  
166 results. This was especially the case for exp. n°2, 3, 5, 7, 8, 12, 13, 14, 15.

167

### 168 **3. Results**

#### 169 **3.1 Diffusion of organic acids in Callovo-Oxfordian clay rock**

170 A comparison between solutes is made in Figure 1 on the normalized fluxes and  
171 downstream cumulative concentration. For more details, the raw experimental data  
172 (downstream flux with precision, downstream cumulative concentration and upstream  
173 concentration) are given in supplementary data and compared with modelling (Fig. S1-S5).  
174 The normalized downstream fluxes (Fig. 1) rise to a plateau, which is representative of the  
175 effective diffusion coefficient of the solute,  $D_e$ . The corresponding values,  $D_e^{ORGA} \sim 10^{-12} \text{ m}^2$   
176  $\text{s}^{-1}$  value (eq. 4), are much lower than effective diffusion coefficient of water ( $D_e^{HTO} > 10^{-11}$   
177  $\text{m}^2 \text{ s}^{-1}$ ). Similar behaviours were evidenced on inorganic anions in sedimentary rocks  
178 (Descostes et al., 2008; Van Loon and Mibus, 2015) as well as for organic acids in Callovo-  
179 Oxfordian clay rock (Dagnelie et al., 2014). The transitory state display various duration,  
180 from almost no retardation (for HTO, Acetate or Adipate), to a significant retardation  
181 observed for EDTA or Oxalate (up to 100 days).

182 The  $D_e$  and  $\alpha$  values adjusted from experimental results (best fit) are gathered in Table  
183 1. When available, the data of reference tracers (HDO, HTO), allow an estimation of  
184 variability from one sample to the other. A variability of a factor 3 is observed on  
185 diffusivities:  $D_e^{HTO}$  ranging from 1.5 to 4.5  $10^{-11} \text{ m}^2 \text{ s}^{-1}$ . It is then much more reliable to

186 compare results normalized by the value of the reference tracer (HDO, HTO). This is  
187 performed by calculation of the factor  $\Pi$  given by the following equation:

188

$$189 \quad \Pi = \frac{[D_e^{ANION}/D_0^{ANION}]}{[D_e^{REF}/D_0^{REF}]} \quad (5)$$

190 Where  $D_e$  is the effective diffusion coefficient in the porous solid and  $D_0$  the diffusion  
191 coefficient in water.  $D_0$  values are corrected from the effect of salinity (I.S.  $\sim 0.105$  eq. in  
192 Callovo-Oxfordian porewater and from Temperature,  $T^{EXP.} \sim 22 \pm 2$  °C). Superscripts refer to  
193 the solutes, which are either anions ( $Cl^-$ , Organic) or neutral references (HTO or HDO). The  
194 ratio:  $\Pi$  isolates the effect of clay on the diffusion pathway of anions (i.e. tortuosity and  
195 constrictivity as discussed by Van Brakel and Heertjes, 1974). For example, a reduced  
196 accessible porosity for anions,  $\epsilon_a$ , induces a lower diffusivity than that of water,  $\Pi < 1$ . Several  
197 empirical observations evidenced this correlation between  $\Pi$  measured in sedimentary rocks  
198 and  $\epsilon_a/\epsilon$ , which is a quantification of the anion exclusion. The most common model is the  
199 empirical Archie's law (Eq. (6), Archie (1942), with  $m \sim 2.4$ ), and further adaptations in  
200 various media, such as m-Archie's law (Eq. (7), Jacquier et al. (2013) with  $\alpha = 0.17$  and  $m =$   
201 1.6) developed for Callovo-Oxfordian clay samples of variable mineralogy, or also e-Archie's  
202 law (Eq. (8), Van Loon et al. (2015), with  $B=10^{-11} \text{ m}^2 \text{ s}^{-1}$ ,  $m_1 = 2.4$  and  $m_2 = 1$ ) adjusted on  
203 low porosity materials ( $\epsilon < 2 \cdot 10^{-2}$ ).

204

$$205 \quad \frac{D_e}{D_0} = \epsilon^m \quad (6)$$

$$206 \quad \frac{D_e}{D_0} = \alpha \times \epsilon^m \quad (7)$$

$$207 \quad D_e = D_0 \times \epsilon^{m_1} + B \times \epsilon^{m_2} \quad (8)$$

208

### 209 **3.2 Effect of Ionic Strength and anion exclusion**

210 Two important features arise from the previous results. First, the low  $\alpha$  ratios for  
211 organic anions in Callovo-Oxfordian clay rock,  $0.1 < \alpha < 0.5$ , traduce a strong but variable  
212 exclusion for these compounds probably originating from charge and or steric effects.  
213 Nevertheless, adsorption occurs for these compounds, and the apparent porosity  $\alpha(\text{orga})$   
214 differs from accessible porosity  $\varepsilon_a(\text{orga})$ , which remains hardly measurable by direct methods.  
215 Thus the parameter  $\alpha$  seems the most reliable and accurate data to quantify an accessible  
216 porosity for organic anions:  $\varepsilon_a(\text{orga})$ . Still, this requires to choose carefully one of the above  
217 the empirical laws, i.e. the most suitable for the studied material.

218 The figure 2 illustrates the diffusivity of chloride, taken as a non sorbing anion in clay-  
219 rich media. It was measured by through-diffusion through Callovo-Oxfordian samples (Blin et  
220 al., 2013) and percolation through compacted illite samples (Chen et al., 2018). The  
221 variability was induced by experimental setup, performed several times under various ionic  
222 strengths. The increase of ionic strength is known to reduce the size of the diffuse layer at the  
223 surface of charged minerals, thus decreasing anion exclusion. This is indeed observed on both  
224  $D_e$  and  $\varepsilon_a$  values and allows a verification of Archie's law as performed in Fig. 2. A  
225 comparison is made with other data from literature on clay rich media (various contents of  
226 illite, smectite and kaolinite minerals). It ensures that the correlation  $\alpha = f(\varepsilon_a/\varepsilon)$  follows  
227 similar trends for all the discussed media. This legitimates further comparison of these  
228 systems and the use of m-Archie law following Eq. (7) (Jacquier et al., 2013) for these results.  
229 This law was used to calculate the  $\varepsilon_a/\varepsilon$  values for organic solutes, and data are reported in both  
230 table 1 and Figure 3.

231

### 232 **3.2 Variability of retardation factor**

233 Only a few studies assess the effect of porosity exclusion on retardation factors in  
 234 clay-rich media. Usually in such media, the Eq. (2) is admitted assuming the following  
 235 hypotheses: i) Adsorption only occurs for cations for which all the porosity is accessible, i.e.  
 236  $\varepsilon(\text{cations}) = \varepsilon$ , ii) Anions, for which  $\varepsilon_a(\text{anions}) < \varepsilon$ , display a negligible adsorption i.e.  $R_d^{APP} =$   
 237 0. This is true for most of the inorganic anions in Callovo-Oxfordian clay rock, but is not true  
 238 for oxoanions or organic anions (Frasca et al., 2014; Rasamimanana et al., 2017). Indeed, the  
 239 organic anions display both properties of adsorption ( $R_d^{APP} > 0$ ) and of anion exclusion  
 240  $\varepsilon_a(\text{orga}) < \varepsilon$ . This latter property possibly induces a modification of the retardation factor. The  
 241 exclusion of solutes from a part of porosity may reduce the accessibility to surfaces and  
 242 eventually lengthen the diffusion pathway (tortuosity). Such effect would decrease the  
 243 apparent adsorption  $R_d^{APP}$  during transport. A similar effect was demonstrated by diffusion of  
 244 solutes in unsaturated samples by Savoye et al. (2012c and 2017). The authors showed that  
 245 the decrease of water-filled porosity was leading to a decrease of Cesium diffusivity and  
 246 adsorption. To quantify such effects on organic anions, we gathered results performed at  
 247 various ionic strengths with  $^{14}\text{C}$ -oxalate and other small carboxylates (data from Chen et al.,  
 248 2018). In this latter case, the  $R_d^{MAX}$  values were calculated by extrapolation of percolation  
 249 results at infinite ionic strength (Fig. S6, table S3). The Fig. 2 illustrates the correlation  
 250 between anion exclusion ( $\varepsilon_a/\varepsilon$ ) and adsorption during transport ( $R_d/R_d^{MAX}$ ). A trend is  
 251 observed and could be adjusted by an exponential law of the following form:

$$252 \quad \frac{R_d^{APP}}{R_d^{MAX}} = f^{CORR} = \frac{1}{\left[1 + \exp\left(a \times \left(b - \frac{\varepsilon_a}{\varepsilon}\right)\right)\right]} \quad (9)$$

253 This empirical law traduces a decrease of  $R_d^{APP}$  with exclusion ( $\varepsilon_a/\varepsilon < 1$ ). The law starts from  
 254 a maximum value,  $R_d^{APP} = R_d^{MAX}$ , in absence of exclusion ( $\varepsilon_a = \varepsilon$ , all surfaces accessible). A  
 255 threshold appears at a value  $\varepsilon_a/\varepsilon = b$ , with a collapse of  $R_d^{APP}$  when  $\varepsilon_a/\varepsilon < b$ . In our case, the  
 256 best fit parameters were  $a = 12.95$  and  $b = 0.60$ . This adjustment remains empirical and such

257 law should be studied in detail for each porous media. However, such behaviour shows  
 258 potential implications which are discussed furtherly. To that aim, the Eq. (7) provides a  
 259 correction factor,  $f^{CORR}$ , leading to a generalized diffusion law:

$$260 \quad \frac{\partial C}{\partial t} = \frac{D_e}{\alpha} \frac{\partial^2 C}{\partial x^2} = \frac{D_e}{\varepsilon \alpha + \rho_g (1 - \varepsilon) f^{CORR} R_d^{CELL}} \frac{\partial^2 C}{\partial x^2} \quad (10)$$

261

## 262 4. Discussion

263 The following discussion assesses the generalized law, Eq. (10), by comparison  
 264 between data from batch and diffusion experiments. The validity of such approach is  
 265 discussed with emphasis on retardation variability and environmental implications.

266

### 267 4.1 Comparison between batch and diffusion experiments

268 The table 1 gathers adsorption data on 15 diffusion experiments, using 8 different  
 269 organic anions of various polarities. Batch data were compare to diffusion data, using the  
 270 following equations:

$$271 \quad R_d^{BATCH} = \frac{1}{L} \int_{x=0}^L R_d \left( \frac{C_0 x}{L} \right) dx = \frac{Q}{C_0} \times \ln(1 + K_L \times C_0) \quad (11)$$

$$272 \quad R_d^{APP} = \frac{(\alpha - \varepsilon_a)}{\rho_g (1 - \varepsilon)} \quad R_d^{CELL} = \frac{(\alpha - \varepsilon_a)}{\rho_g (1 - \varepsilon) f^{CORR} \left( \frac{\varepsilon_a}{\varepsilon} \right)} \quad (12)$$

273 The Eq. (11) traduces the adsorption expected in diffusion experiment, calculated  
 274 thanks to batch data. A linear concentration profile along the diffusion cell is assumed,  $C(x) =$   
 275  $C_0 \times [x/L]$ , and averaged using the Langmuir law, defined in Eq.1:  $R_d(C) = f(Q, K_L, C)$ .

276 The Eq. (12) traduces the adsorption directly extrapolated from diffusion data, using  
 277 the adjusted apparent porosity,  $\alpha$ , with (eq. 2) or without (eq. 10) the correction factor defined  
 278 above.

279 The Figure 4 illustrates the comparison between batch and diffusion data. The red  
280 triangles show  $R_d^{APP}$  as a function of  $R_d^{BATCH}$ . Using raw batch data may lead to a significant  
281 overestimation of apparent porosity and retardation factor. The green triangles show  $R_d^{CELL}$  as  
282 a function of  $R_d^{BATCH}$ . A fairly good agreement is observed between batch data and diffusion  
283 data corrected from exclusion effects. The proposed correction factor is only a rough  
284 empirical adjustment, and no tool for accurate prediction of retardation factors. However, it  
285 strengthens the hypothesis of porosity exclusion as the key parameter affecting diffusive  
286 retardation. This feature would explain various effects observed on several species. For  
287 example, ionic strength effects are observed in the case of oxalate with the decrease of  $\alpha$  and  
288  $R_d^{APP}$  by a factor 2 when ionic strength increases between Exp. n°7 and 8. Also a large  
289 difference of retardation was observed between Eu-EDTA and EDTA species. This would be  
290 explained by a higher exclusion of the latter, as quantified by  $D_e$  values. This specific case  
291 leads to the following discussion on the origin of exclusion.

292

#### 293 **4.2 Origin of exclusion from the porosity**

294 An interesting feature is the origin of the exclusion of adsorbates. Two specific effects  
295 are viewed in this study: i.e. steric and charge effects. It seems clear that formal charge is not  
296 a good indicator of electrostatic effects, as observed with inorganic anions (Descostes et al.,  
297 2008; Wigger and Van Loon, 2017). Still, charge effects are expected in clay rich media, and  
298 most probably linked to charge density, polarizability, or even hardness of anionic Lewis  
299 bases. Such assumption can be made in view of experimental results. For example, the  
300 diffusion of small anion  $NO_3^-$  in Callovo-Oxfordian clay rock, displayed a much lower  
301 exclusion than for  $Cl^-$ ,  $\Pi(NO_3^-) \sim 0.7 \gg \Pi(Cl^-) \sim 0.4$  (Dagnelie et al., 2017). This result  
302 agrees with a lower exclusion of  $NO_3^-$ , of which charge is distributed between 3 atoms  
303 compared to  $Cl^-$ . In the present study also, the values  $\Pi(oxalate) \sim 0.25-0.36$  were lower than

304  $\Pi(\text{o-phthalate}) \sim 0.1-0.25$ , despite a larger size for the latter. This also indicates possible  
305 charge effects in addition to steric effects. Yet, it is not clear for organic anions, which parts  
306 of exclusion are due to charge effect and steric effect. In addition to charge exclusion, larger  
307 molecule may be more excluded from porosity, due to the presence of small porosity in clay  
308 rich media (Gaboreau et al., 2016; Wigger and Van Loon, 2018). Such hypothesis seems  
309 confirmed by the correlation between  $\Pi$  and molecule size (Fig. S7). Obviously, such  
310 relationship remains a trend rather than a well-defined correlation, given that two factors are  
311 simultaneously involved, i.e. charge and size. Further studies would be interesting to  
312 decorrelate both effects using molecules of well-known properties. To that aim,  $D_e$  and  $\Pi$   
313 values should be measured more accurately and preferentially on the same sample. Also  
314 molecular size should take into account speciation in solution and hydration shell of species.  
315 Finally, additional modelling seem mandatory to quantify relevant electric properties of  
316 adsorbates (charge density, shape and energy of the highest occupied molecular orbital, etc..).

317

### 318 **4.3 Methodology and environmental implications**

319 The easiest method to quantify adsorption involves usually batch experiments on  
320 crushed samples. Such approach is commonly preferred to diffusion experiments, much more  
321 time consuming, or percolation experiments involving other processes and possible bias  
322 (advection, dispersion, minerals leaching). The previous findings highlight the difficulty to  
323 predict retardation factors in clay-rich media only based on adsorption data, especially for  
324 organic anions. A generalized law is proposed for adsorption-diffusion with equation (10). It  
325 is in agreement with classical laws for cations and non-sorbing anions. In the case of  
326 adsorbing anions, it includes an additional effect due to porosity exclusion. This effect should  
327 be studied first, in order to assess the shape of  $f^{\text{CORR}}(\epsilon_a/\epsilon)$  curve. This empirical factor does  
328 not exempt from performing diffusion experiments, as they provide the most accurate



329 estimation  $\alpha$  parameter. In addition, the quantification of  $D_e/D_0$  also seems mandatory to get  
330 an estimation of the exclusion of sorbing anions,  $\epsilon_a/\epsilon$ . To that aim, the use of an inert tracer  
331 (HTO, HDO) as reference is highly recommended, since  $D_e$  values display a variability of a  
332 factor 2 to 3 among similar samples. Also the extrapolation of  $\epsilon_a/\epsilon$  using  $D_e/D_0$  value requires  
333 the choice an Archie's-type law suitable for the material.

334 In the case of clay rocks, a low diffusivity for organic anions is evidenced with  $D_e$   
335 values ranging between 0.8 and  $7 \cdot 10^{-12} \text{ m}^2 \text{ s}^{-1}$ . The adsorption properties might lead to high  
336 apparent porosity as observed for oxalate or ISA. However, the species with lowest  
337 diffusivities,  $D_e < 2 \cdot 10^{-12} \text{ m}^2 \text{ s}^{-1}$  may present an important anion exclusion leading to a  
338 strongly reduced retardation. Similar methodologies should be suitable in other material but  
339 taking account of the media specificity. Depending on the materials, sorbing or non-sorbing  
340 species differs leading to various reference solutes (Schaffer et al., 2017). It would be  
341 interesting to perform such comparative studies on various media such as oxisoils, sediments  
342 or cementitious materials.

343

## 344 **5. Conclusions**

345 In this study we evaluated diffusive data of eight organic anions through Callovo-  
346 Oxfordian clay rock, a clay-rich sedimentary rock. The affinities of organic anions for rock  
347 surfaces induced various retardation factors. However, a significant discrepancy was observed  
348 between maximum adsorption data measured by batch experiments and apparent adsorption  
349 extrapolated from diffusive retardation. A qualitative explanation is proposed based on  
350 porosity exclusion, probably due to both steric and charge effects. The decrease of accessible  
351 porosity for a solute may modify accessible surface or tortuosity, thus leading to a reduced  
352 retardation. This was observed on both compacted clay minerals and Callovo-Oxfordian clay  
353 rock. A threshold value of  $\epsilon_a/\epsilon$  is eventually observed under which the retardation of sorbing

354 species collapses. This feature should be assessed and valuate for each specific solute/media  
355 couple. This may be achieved in the case sorbing anions in clay-rich media, using various  
356 ionic strengths, which impact both accessible porosity and retardation factor.

357 In a first approximation, an empirical correction factor  $[1/(1+a \times \exp(b - \epsilon_a/\epsilon))]$  was  
358 proposed. This factor estimates the ratio between apparent and maximum adsorption during  
359 migration in a porous media. It was evaluated for Callovo-Oxfordian clay rock thanks to  
360 diffusion data and percolation through compacted illite. The parameters  $a = 12.95$  and  $b = 0.60$   
361 were adjusted and used to estimate adsorption from 15 diffusion experiments. A reasonable  
362 agreement was observed between adsorption experiments in batches and diffusion  
363 experiments in cell. The low diffusivity of organic species is confirmed, with  $D_e$  values  
364 ranging between  $0.5$  and  $7 \cdot 10^{-12} \text{ m}^2 \text{ s}^{-1}$ . These values traduce anion exclusion from porosity  
365 probably due to charge and possibly with additional steric effects. The effective diffusion was  
366 necessary to evaluate the accessible porosity (anion exclusion), following m-Archie law.  
367 Finally, a significant retardation was observed for several species, such as oxalate of ISA.  
368 Still, this retardation factor strongly decreased for the most excluded species, i.e. with values  
369  $\epsilon_a/\epsilon \ll b = 0.60$ , or  $D_e < 2 \cdot 10^{-12} \text{ m}^2 \text{ s}^{-1}$ .

370 The proposed methodology should be applicable to other media with charged surfaces  
371 such as cementitious materials or oxisoils. It would be interesting to compare such results,  
372 since the solutes affinity or exclusion will differ from one media to the other. Such approach  
373 could help assessing the transport of organic solutes in the environment.

374

### 375 **Acknowledgments**

376 In memory of Dr. Eric Giffaut. This work was partially financed by the National Radioactive  
377 Waste Management Agency (Andra). We thank F. Goutelard for early diffusive experiments at

378 various ionic strength. We gratefully thank two anonymous reviewers for their constructive  
379 comments and suggestions.

380

## 381 **References**

382 Archie, G.E., 1942. The electrical resistivity log as an aid in determining some reservoir  
383 characteristics. *Trans. AIME* 146, 54–62.

384 Banzhaf, S., Hebig, K., 2016. Use of column experiments to investigate the fate of organic  
385 micropollutants - a review. *Hydrol. Earth Syst. Sci.*, 20, 3719–3737.

386 Bazer-Bachi, F., Descostes, M., Tevissen, E., Meier, P., Grenut, B., Simonnot, M.-O. Sardin,  
387 M. 2007. Characterization of sulphate sorption on Callovo-Oxfordian argillites by batch,  
388 column and through-diffusion experiments, *Physics and Chemistry of the Earth, Parts A/B/C*,  
389 32, 8–14.

390 Blin, V., Arnoux, P., Hainos, D., Radwan, J., 2013. Influence of a saline plume (NaNO<sub>3</sub>) on  
391 radionuclide mobility in the Callovo-Oxfordian clay rock. *Radionuclide Migration*  
392 *Conference*, 2013 09 08-13, Brighton, UK.

393 Borisover, M., Graber, E.R., 1997. Specific interaction of Organic compounds with soil  
394 organic carbon. *Chemosphere* 34, 8, 1761-1776.

395 Borisover, M., Davis, J., 2015. Adsorption of inorganic and organic solutes by clay minerals.  
396 in: Tournassat, C., Steefel, C., Bourg, I.C., Bergaya, F. (Eds.), *Natural and Engineered Clay*  
397 *Barriers*. Elsevier.

398 Brusseau, M.,L., 1991. Nonequilibrium Sorption of Organic Chemicals: Elucidation of Rate-  
399 Limiting Processes. *Environ. Sci. Technol.* 25, 134-142.

400 Charlet, L., Alt-Epping, P., Wersin, P., Gilbert, B., 2017. Diffusive transport and reaction in  
401 clay rocks: A storage (nuclear waste, CO<sub>2</sub>, H<sub>2</sub>), energy (shale gas) and water quality issue.  
402 *Adv. Water Res.* 106, 39-59.

403 Chen, Y., Glaus, M.A., Van Loon, L.R., Mäder, U. 2018. Transport of low molecular weight  
404 organic compounds in compacted illite and kaolinite. *Chemosphere* 198, 226-237.

405 Curtis, G.P., Roberts, P.V., Reinhard, M. 1986. A Natural Gradient Experiment on Solute  
406 Transport in a Sand Aquifer 4. Sorption of Organic Solutes and its Influence on Mobility.  
407 *Wat. Res. Research* 22, 13, 2059-2067.

408 Crank, J., 1975. *The Mathematics of Diffusion*. Clarendon Press, London.

409 Dagnelie, R.V.H., Arnoux, P., Radwan, J., Lebeau, D., Nerfie, P., Beaucaire, C., 2015.  
410 Perturbation induced by EDTA on HDO, Br<sup>-</sup> and Eu<sup>III</sup> diffusion in a large-scale clay rock  
411 sample. *Appl. Clay Sci.* 105-106, 142–149.

412 Dagnelie, R.V.H., Descostes, M., Pointeau, I., Klein, J., Grenut, B., Radwan, J., Lebeau, D.,  
413 Georgin, D., Giffaut, E., 2014. Sorption and diffusion of organic acids through clayrock:  
414 comparison with inorganic anions. *J. Hydrol.* 511, 619-627.

415 Dagnelie, R.V.H., Rasamimanana, S., Thory, E., Lefèvre, G., 2017. Competitive adsorption of  
416 organic molecules on sediments. *Procedia Earth Plan. Sci.* 17, 144-147.

417 Delage, P., Cui., Y.J., Tang, M., 2010. Clays in radioactive waste disposal. *J. Rock. Mech.*  
418 *And Geotech. Eng.* 2 (2), 111-123.

419 Descostes, M., Blin, V., Bazer-Bachi, F., Meier, P., Grenut, B., Radwan, J., Schlegel, M.L.,  
420 Buschaert, S., Coelho, D., Tevissen, E., 2008. Diffusion of anionic species in Callovo-  
421 Oxfordian argillites and oxfordian limestones (Meuse/Haute-Marne, France). *Appl. Geochem.*  
422 23, 655–677.

423 Descostes, M., Pointeau, I., Radwan, J., Poonosamy, J., Lacour, J.-L., Menut, D., Vercouter,  
424 T., Dagnelie, R.V.H. , 2017. Adsorption and retarded diffusion of Eu<sup>III</sup>-EDTA<sup>-</sup> through hard  
425 clay rock. *J. Hydrol.* 544,125-132.

426 Duarte, R., Matos, J., Senesi, N., 2018. Chapter 5 - Organic Pollutants in Soils, In *Soil*  
427 *Pollution*, edited by A. C. Duarte, A. Cachada and T. Rocha-Santos, Academic Press, 103–

428 126.

429 Durce, D., Landesman, C., Grambow, B., Ribet, S., Giffaut, E., 2014. Adsorption and  
430 transport of polymaleic acid on Callovo-Oxfordian clay stone: batch and transport  
431 experiments. *J. Contam. Hydrol.* 164, 308-322.

432 Frasca, B., Savoye, S., Wittebroodt, C., Leupin, O.X., Descostes, M., grenut, B., Etep-  
433 Batanken, J., Michelot, J-L., 2012. Influence of redox conditions on iodide migration  
434 through a deep clay formation (Toarcian argillaceous rock, Tournemire, France). *Appl.*  
435 *Geochem.* 27, 2456-2462.

436 Frasca, B., Savoye, S., Wittebroodt, C., Leupin, O.X., Michelot, J.-L., 2014. Comparative  
437 study of Se oxyanions retention on three argillaceous rocks: Upper Toarcian (Tournemire,  
438 France), Black Shales (Tournemire, France) and Opalinus Clay (Mont Terri, Switzerland). *J.*  
439 *Environ. Rad.* 127, 133-140.

440 Gaboreau, S., Robinet, J.-C., Prêt, D., 2016. Optimization of pore-network characterization of  
441 a compacted clay material by TEM and FIB/SEM imaging. *Microp. Mesopo. Materials* 224,  
442 116-128.

443 Gaucher, E., Robelin, C., Matray, J., Negrel, G., Gros, Y., Heitz, J., Vinsot, A., Rebours, H.,  
444 Cassagnabère, A., Bouchet, A., 2004. ANDRA underground research laboratory:  
445 interpretation of the mineralogical and geochemical data acquired in the Callovo-Oxfordian  
446 formation by investigative drilling. *Phys. Chem. Earth* 29, 55-77.

447 Hummel, W., 2008. Radioactive contaminants in the subsurface: the influence of complexing  
448 ligands on trace metal speciation. *Monatshefte für Chemie – Chem. Mon.* 139, 459–480.

449 Jacquier, P., Hainos, D., Robinet, J.-C., Herbette, M., Grenut, B., Bouchet, A., Ferry, C.,  
450 2013. The influence of mineral variability of Callovo-Oxfordian clay rocks on radionuclide  
451 transfer properties. *Applied Clay Sci.* 83-84, 129-136.

452 Keith-roach, M.J., 2008. The speciation, stability, solubility and biodegradation of organic co-  
453 contaminant radionuclide complexes: A review. *Sci. Total Environ.* 96, 1–11.

454 Keller, A.A., Wang, H., Zhou, D., Lenihan, H.S., Cherr, G., Cardinale, B.J., Miller, R., Ji, Z.,  
455 2010. Stability and Aggregation of Metal Oxide Nanoparticles in Natural Aqueous Matrices  
456 *Environ. Sci. Technol.* 44 (6), 1962–1967.

457 Lerouge, C., Grangeon, S., Gaucher, E.C., Tournassat, C., Agrinier, P., Guerrot, C. Widory,  
458 D., Fléhoc, C., Wille, G., Ramboz, C., Vinsot, A., Buschaert, S., 2011. Mineralogical and  
459 isotopic record of biotic and abiotic diagenesis of the Callovo-Oxfordian clayey formation of  
460 Bure (France). *Geochim. Cosmochim. Acta* 75 (10), 2633-2663.

461 Liu, H., Chen, T., Frost, R.L., 2014. An overview of the role of goethite surfaces in the  
462 environment. *Chemosphere* 103, 1-11.

463 Melkior, T., Yahiaoui, S., Thoby, D., Motellier, S., Barthes, V., 2007. Diffusion coefficients  
464 of alkaline cations in Bure mudrock. *Phys. Chem. Earth Parts A/B/C* 32, 453–462.

465 Montavon, G., Sabatié-Gogova, A., Ribet, S., Bailly, C., Bessaguet, N., Durce, D., Giffaut, E.,  
466 Landesman, C., Grambow, B., 2014. Retention of iodide by the Callovo-Oxfordian formation:  
467 An experimental study. *Appl. Clay Sci.* 87, 142–149.

468 Moridis, G.J., 1998. A Set of semianalytical solutions for parameter estimation in diffusion  
469 cell experiments. *Sci. York*.

470 Nowack, B., Xue, H., Sigg, L. 1997. Influence of Natural and Anthropogenic Ligands on  
471 Metal Transport during Infiltration of River Water to Groundwater. *Environ. Sci. Technol.* 31,  
472 866-872.

473 Pellenard, P., Deconinck, J.-F., 2014. Mineralogical variability of callovo-oxfordian clays  
474 from the paris basin and the subalpine basin. *C.R. Geosci.* 338, 854-866.

475 Rasamimanana, S. Rétenion et transport diffusif d’anions organiques dans la roche argileuse  
476 du Callovo-Oxfordien ; Ph.D. Thesis, Université Pierre et Marie Curie Paris-VI, France, 2016.

477 Rasamimanana, S., Lefèvre, G., Dagnelie, R., 2017. Various causes behind desorption  
478 hysteresis of carboxylic acids on mudstones. *Chemosphere* 168, 559-567.

479 Read, D., Ross, D., Sims, R.J. 1998. The migration of uranium through Clashach Sandstone:  
480 the role of low molecular weight organics in enhancing radionuclide transport. *J. Contam.*  
481 *Hydrol.* 35, 235-248.

482 Ren, X., Zeng, G., Tang, L., Wang, J., Wan, J., Liu, Y., Yu, J., Yi, H., Ye, S., Deng, R., 2018.  
483 Sorption, transport and biodegradation – An insight into bioavailability of persistent organic  
484 pollutants in soil. *Sci. Total Environ.* 610–611, 1154-1163.

485 Roberts, P.V., Goltz, M.N., Mackay, D.M. 1986. A Natural Gradient Experiment on Solute  
486 Transport in a Sand Aquifer 3. Retardation Estimates and Mass Balances for Organic Solutes.  
487 *Wat. Res. Research* 22, 13, 2047-2058.

488 Roy, S.B., Dzombak, D.A. 1998. Sorption nonequilibrium effects on colloid-enhanced  
489 transport of hydrophobic organic compounds in porous media. *J. Contam. Hydrol.* 30, 179-  
490 200.

491 Savoye, S., Goutelard, F., Beaucaire, C., Charles, Y., Fayette, A., Herbette, M., Larabi, Y.,  
492 Coelho, D., 2011. Effect of temperature on the containment properties of argillaceous rocks:  
493 The case study of Callovo–Oxfordian claystones. *J. Contam. Hydrol.* 125, 102-112.

494 Savoye, S., Beaucaire, C., Fayette, A., Herbette, M., Coelho, D., 2012a. Mobility of cesium  
495 through the Callovo-Oxfordian claystones under partially saturated conditions. *Environ. Sci.*  
496 *Technol.* 46, 2633–2641.

497 Savoye, S., Frasca, B., Grenut, B., Fayette, A., 2012b. How mobile is iodide in the Callovo–  
498 Oxfordian claystones under experimental conditions close to the in situ ones?, *J. Contam.*  
499 *Hydrol.* 142–143, 82-92.

500 Savoye, S., Beaucaire, C., Fayette, A., Herbette, M., Coelho, D., 2012c. Mobility of Cesium  
501 through the Callovo-Oxfordian Claystones under Partially Saturated Conditions. *Envir. Sci.*

502 Tech. 46, 2633-2641.

503 Savoye, S., Beaucaire, C., Grenut, B., Fayette, A., 2015. Impact of the solution ionic strength  
504 on strontium diffusion through the Callovo-Oxfordian clayrocks: an experimental and  
505 modelling study. *Appl. Geochem.* 61, 41–52.

506 Savoye, S., Lefèvre, S., Fayette, A., Robinet, J.-C., 2017. Effect of Water Saturation on the  
507 Diffusion/Adsorption of  $^{22}\text{Na}$  and Cesium onto the Callovo-Oxfordian Claystones. *Geofluids*.  
508 1683979, 17p.

509 Schaffer, M., Licha, T., 2015. A framework for assessing the retardation of molecules in  
510 groundwater: Implications of the species distribution for the sorption-influenced transport.  
511 *Sci. Total Environ.* 524-525, 187-194.

512 Schaffer, M., Warner, W., Kutzner, S., Börnick, H., Worch, E., Licha, T., 2017. Organic  
513 molecules as sorbing tracers for the assessment of surface areas in consolidated aquifer  
514 systems. *J. Hydrology*, 546, 370-379.

515 Szecsody, J.E., Zachara, J.M., Chilakapati, A., Jardine, P.M., Ferency, A.S., 1998.  
516 Importance of flow and particle-scale heterogeneity on  $\text{Co}^{\text{II/III}}$  EDTA reactive transport. *J.*  
517 *Hydrol.* 209, 112–136.

518 Tournassat, C., Steefel, C. I., Bourg, I. C., Bergaya, F. Editor(s), *Natural and Engineered Clay*  
519 *Barriers*, In *Developments in Clay Science*, Elsevier, 2015. 6, 1572-4352.

520 Van Loon, L.R., Mibus, J., 2015. A modified version of Archie's law to estimate effective  
521 diffusion coefficients of radionuclides in argillaceous rocks and its application in safety  
522 analysis studies. *Applied Geochem.* 59, 85-94.

523 Vinsot, A., Anthony, C., Appelo, J., Lundy, M., Wechner, S., Cailteau-Fischbach, C., de  
524 Donato, P., Pironon, J., Lettry, Y., Lerouge, C., De Cannière, P., 2017. Natural gas extraction  
525 and artificial gas injection experiments in Opalinus Clay, Mont Terri rock laboratory  
526 (Switzerland). *Swiss J. Geosci.* 110, 375-390.



527 Weber, W.J.Jr., McGinley, P.M., Katz, L.E. 1991. Sorption phenomena in subsurface  
528 systems: concepts, models and effects on contaminant fate and transport. *Wat. Res.* 25, 5,  
529 499-528.

530 Wigger, C., Gimmi, T., Muller, A., Van Loon, L.R., 2018. The influence of small pores on the  
531 anion transport properties of natural argillaceous rocks – A pore size distribution investigation  
532 of Opalinus Clay and Helvetic Marl. *Applied Clay Sci.* 156, 134-143.

533 Wigger, C., Van Loon, L.R., 2017. Importance of interlayer equivalent pores for anion  
534 diffusion in clay-rich sedimentary rocks. *Environ. Sci. Technol.* 51 (4), 1998–2006.

535 Zachara, J.M., Gassman, P.L., Smith, S.C., Taylor, D., 1995. Oxidation and adsorption  
536 of Co(II) EDTA<sup>2-</sup> complexes in subsurface materials with iron and manganese oxide grain  
537 coatings. *Geochim. Cosmochim. Acta* 59, 4449–4463.

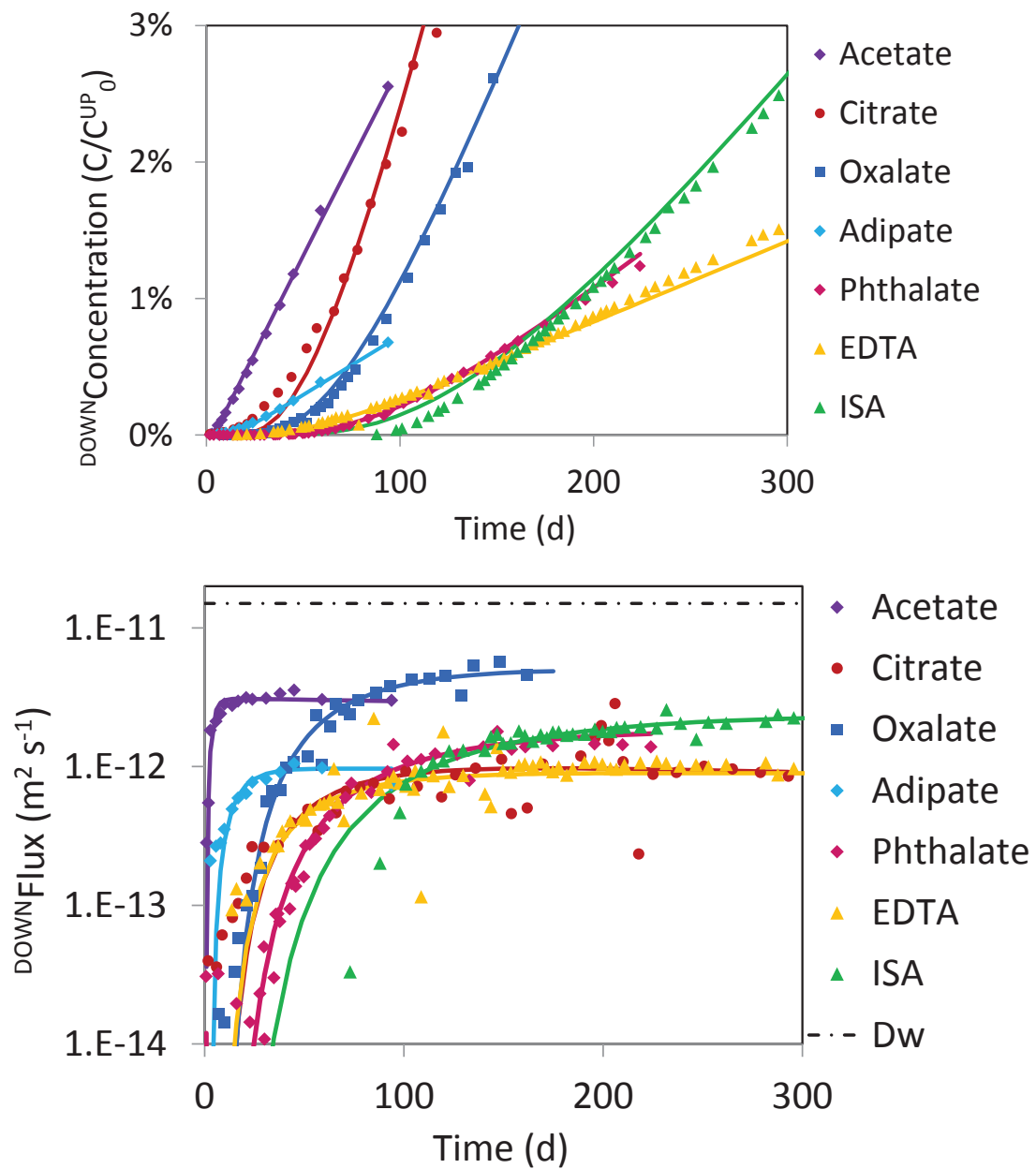
**Figure**[Click here to download Figure: Figure 1 - Flux.docx](#)

Figure 1: Illustration of diffusion experimental results.

Signs represent experimental data and solid curve represent best fit modelling. (Top) Downstream concentration as a function of time. Values normalized by initial upstream concentration.

(Bottom) Normalized downstream flux used for parametric adjustment.

$D_w$  indicates the minimum  $D_e$  value measured for water:  $D_e^{\text{MIN}}(\text{HTO}) = 15 \cdot 10^{-11} \text{ m}^2 \text{ s}^{-1}$ .

**Figure**

[Click here to download Figure: Figure 2 - Effet exclusion De.docx](#)

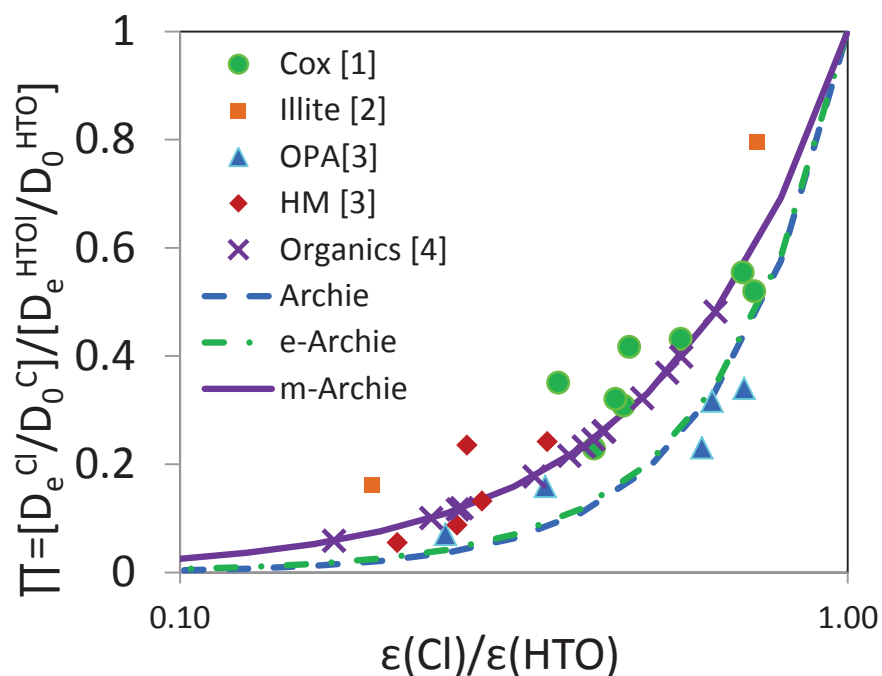


Figure 2: Effect of anion exclusion on diffusion parameters of chloride (Cl<sup>-</sup>). [1] Cl<sup>-</sup> diffusion in COx at various Ionic strengths. (Unpublished, CEA/Andra, internal report) [2] Percolation experiments in compacted illite (Chen et al., 2018). [3] Diffusion experiments in Opalinus Clay (OPA) and Helvetic Marl (HM) (Wigger and van Loon, 2017). [4] Crosses represent  $\Pi$  values of organics measured in this study. Values were used to extrapolate  $\epsilon_a/\epsilon$  according to an m-Archie law (Jacquier et al., 2013).

**Figure**

[Click here to download Figure: Figure 3 - Effet exclusion Rd.docx](#)

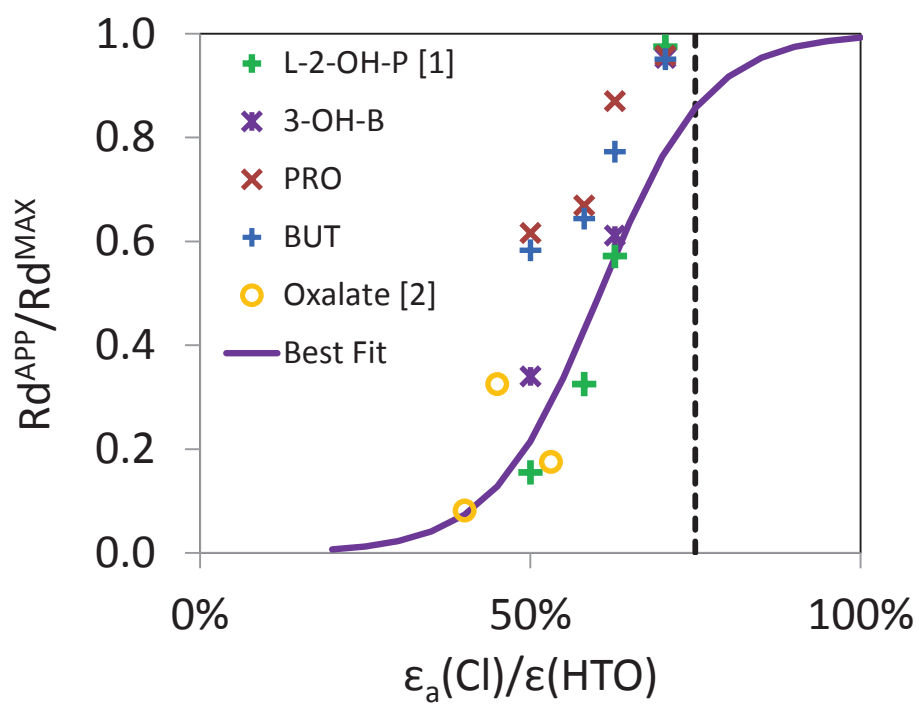


Figure 3: Effect of anion exclusion on adsorption of carboxylic acids in clay rich media.

[1] Percolation in compacted illite (Chen et al., 2018;  $R_d^{MAX}$  extrapolated at high ionic strength).

[2] Diffusion in Callovo-Oxfordian clay rock (This study,  $R_d^{MAX}$  measured by batch experiments).

Solid curve, best fit performed with all experimental data.

Dashed line represents the maximum  $\epsilon_a/\epsilon$  values reached at high ionic strength.

**Figure**

[Click here to download Figure: Figure 4 - Rd batch cell.docx](#)

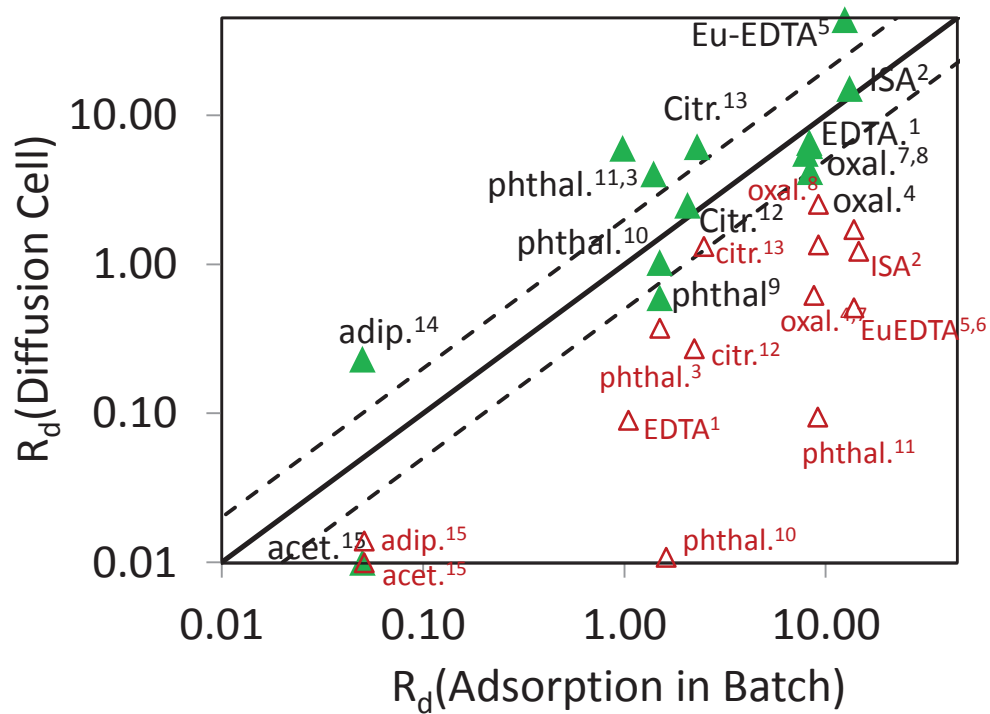


Figure 4: Comparison between  $R_d$  values calculated from diffusion experiments (Y axis) and  $R_d$  values measured by batch experiments (X axis). Superscripts indicate number of the diffusion experiment. Diffusion results are calculated using Eq. (12), leading to  $R_d^{\text{APPARENT}}$  (red empty triangles) or  $R_d^{\text{CORRECTED}}$  (green triangles) calculated with a correction factor (Eq. (9), Fig. 3).

Table 1. Diffusion parameters adjusted from experiments. Taken from [a] Dagnelie et al., 2014 [b] Descostes et al., 2017, [c] this work.

Data in italic were not available and taken from average on similar samples. Data in bold are calculated using eq. 6, 7, 9 &amp; 10.

n°/ref	Tracer	$D_e^{\text{HTO}}$ ( $\text{m}^2 \text{s}^{-1}$ )	$\varepsilon^{\text{HTO}}$ (%)	$D_e^{\text{ORGA}}$ ( $\text{m}^2 \text{s}^{-1}$ )	$\alpha^{\text{ORGA}}$ ( $\text{}$ )	$\Pi^{\text{ORGA}}$	$\varepsilon_a^{\text{ORGA}}$ ( $\text{}$ )	$R_d^{\text{APP}}$ ( $\text{L kg}^{-1}$ )	$R_d^{\text{CELL}}$ ( $\text{L kg}^{-1}$ )	$R_d^{\text{BATCH}}$ ( $\text{L kg}^{-1}$ )
1 [a]	$^{14}\text{C}$ -EDTA	<i>3.60E-11</i>	<i>18.0%</i>	8.90E-13	0.25	<b>1.16E-01</b>	<b>0.047</b>	<b>0.1</b>	<b>6.5</b>	<b>8.3</b>
2 [a]	$^{14}\text{C}$ - $\alpha$ -ISA	<i>3.60E-11</i>	<i>18.0%</i>	2.97E-12	2.60	<b>2.33E-01</b>	<b>0.072</b>	<b>1.1</b>	<b>15.1</b>	<b>13.2</b>
3 [a]	$^{14}\text{C}$ -Phthalate	<i>3.60E-11</i>	<i>18.0%</i>	2.50E-12	0.86	<b>2.46E-01</b>	<b>0.075</b>	<b>0.4</b>	<b>4.0</b>	<b>1.4</b>
4 [a]	$^{14}\text{C}$ -Oxalate	<i>3.60E-11</i>	<i>18.0%</i>	3.80E-12	1.37	<b>2.61E-01</b>	<b>0.078</b>	<b>0.6</b>	<b>5.5</b>	<b>7.9</b>
5 [b]	Eu-EDTA	<i>3.60E-11</i>	<i>18.0%</i>	1.36E-12	3.57	<b>1.78E-01</b>	<b>0.061</b>	<b>1.6</b>	<b>43.6</b>	<b>12.5</b>
6 [b]	$^{152}\text{Eu}$ -EDTA	<i>3.60E-11</i>	<i>18.0%</i>	4.50E-13	1.10	<b>5.88E-02</b>	<b>0.031</b>	<b>0.5</b>	<b>104.3</b>	<b>12.5</b>
7 [c]	$^{14}\text{C}$ -Oxalate	4.42E-11	22.7%	6.60E-12	2.74	<b>3.69E-01</b>	<b>0.122</b>	<b>1.3</b>	<b>4.2</b>	<b>8.4</b>
8 [c]	$^{14}\text{C}$ -Oxalate	3.73E-11	22.9%	6.02E-12	4.97	<b>3.99E-01</b>	<b>0.129</b>	<b>2.3</b>	<b>6.2</b>	<b>8.4</b>
9 [c]	$^3\text{H}$ -Phthalate	2.67E-11	17.9%	9.30E-13	0.07	<b>1.23E-01</b>	<b>0.048</b>	<b>0.01</b>	<b>0.6</b>	<b>1.5</b>
10 [c]	$^3\text{H}$ -Phthalate	4.51E-11	19.5%	1.28E-12	0.07	<b>1.00E-01</b>	<b>0.046</b>	<b>0.01</b>	<b>1.0</b>	<b>1.5</b>
11 [c]	$^3\text{H}$ -Phthalate	2.50E-11	13.0%	8.40E-13	0.24	<b>1.19E-01</b>	<b>0.034</b>	<b>0.1</b>	<b>6.0</b>	<b>1.0</b>
12 [c]	$^{14}\text{C}$ -Citrate	1.80E-11	15.0%	1.19E-12	0.66	<b>2.60E-01</b>	<b>0.065</b>	<b>0.3</b>	<b>2.5</b>	<b>2.1</b>
13 [c]	$^{14}\text{C}$ -Citrate	2.20E-11	18.0%	1.80E-12	2.80	<b>3.22E-01</b>	<b>0.089</b>	<b>1.2</b>	<b>6.1</b>	<b>2.3</b>
14 [c]	$^3\text{H}$ -Acetate	1.50E-11	15.0%	3.20E-12	0.07	<b>4.82E-01</b>	<b>0.095</b>	<b>0.01</b>	<b>0.01</b>	<b>&lt;0.1</b>
15 [c]	$^3\text{H}$ -Adipate	1.50E-11	15.0%	9.80E-13	0.09	<b>2.15E-01</b>	<b>0.057</b>	<b>0.01</b>	<b>0.2</b>	<b>&lt;0.1</b>